Metal-polymer nanocomposite with stable plasmonic tuning under cyclic strain conditions

Chloé Minnai, and Paolo Milani

Citation: Appl. Phys. Lett. **107**, 073106 (2015); doi: 10.1063/1.4928725
View online: https://doi.org/10.1063/1.4928725
View Table of Contents: http://aip.scitation.org/toc/apl/107/7
Published by the American Institute of Physics

Metal-polymer nanocomposite with stable plasmonic tuning under cyclic strain conditions

Chloé Minnai and Paolo Milani[a)]
CIMAINA and Dipartimento di Fisica, Università degli Studi di Milano, via Celoria 16, 20133 Milano, Italy

(Received 26 June 2015; accepted 6 August 2015; published online 17 August 2015)

We report the fabrication and characterization of stretchable nanocomposite films with mechanically tunable surface plasmon resonance. The films have been produced by implantation in a Polydimethylsiloxane substrate of neutral gold nanoparticles aerodynamically accelerated in a supersonic expansion. Optical absorption spectroscopy shows that uniaxial stretching of the nanocomposite induce a reversible redshift of the plasmon peak up to 180 nm from the peak wavelength of the non-stretched sample. The range of the plasmon peak shift depends upon the density of implanted nanoparticles. The optical behavior of the nanocomposite evolves upon cyclical stretching due to the rearrangement of the nanoparticles in the elastomeric matrix. We have identified the fabrication and post-deposition treatment conditions to stabilize the plasmonic shift upon cyclical stretching in order to obtain robust and large area nanocomposites with tunable and reproducible optical properties over a wide visible wavelength range. © *2015 AIP Publishing LLC*.
[http://dx.doi.org/10.1063/1.4928725]

Metal nanoparticles show localized surface plasmon resonances (LSPRs) consisting in a collective oscillation of conduction electrons excited by an electromagnetic field;[1] the localization of the field in structures of nanometric dimensions has profound consequences on light amplification and manipulation due to the fact that changes in nanoparticle volume and/or shape can affect dramatically the optical properties.[1,2] LSPRs in Au and Ag nanoparticles are of particular interest, in view of applications, since their frequency spans a wide spectral range from the visible to the near infrared.[3,4]

Plasmonic nanocomposites consisting of Au or Ag nanoparticles embedded in a dielectric matrix are increasingly used for selective light absorption and/or transmission in optoelectronics, biosensing, and solar energy harvesting.[5–10] The tuning of their optical properties can be obtained by selecting nanoparticle dimensions and geometries, particle density, and hence inter-particle distance.[3,4] This passive tuning requires the preparation of the ingredients of the nanocomposite with predetermined characteristics prior to the fabrication. Active tuning has been recently demonstrated where the plasmonic properties of a nanocomposite are continuously modified by mechanic deformation of the nanoparticle-matrix system in order to change the inter-particle distance and hence select different spectral absorption regions.[11–13] Deformable nanocomposites have been reported to show plasmonic shifts up to around 70 nm for uniaxial deformations of about 20%.[11]

Elastomeric matrices represent simple, low-cost, and effective media for the fabrication of mechanically tunable plasmonic nanocomposites by *in situ* doping with precursors from chemical reduction or physical vapor deposition.[14–16] An alternative approach is based on the mixing of preformed nanoparticles in a solvent subsequently used to prepare the polymer.[17,18] These methods present several weaknesses such as the poor control of spatial distribution and aggregation of the dispersed nanoparticles, not to mention the limited amount of nanoparticles that can be dispersed without negatively affecting the polymerization process of the matrix.[15] The functionalization of elastomeric surfaces with noble metal nanoparticles has been proposed as an alternative to obtain stretchable plasmonic nanocomposites: this approach allows a very precise control of nanoparticle size and reciprocal distance; however, surface-functionalized elastomers are quite fragile and their stability has not yet been characterized.[11–13]

In view of applications, a fundamental issue is the stability of the nanocomposite optical properties upon cyclic strain conditions; to date, no characterization of this aspect is reported in the literature, although there are clear evidences that nanoparticles in an elastomeric matrix are a dynamic system undergoing rearrangement and reorganization upon stretching.[19]

Recently, we showed that neutral metal clusters produced in the gas phase and aerodynamically accelerated by a supersonic expansion can be implanted in a Polydimethylsiloxane (PDMS) substrate to obtain a nanocomposite with superior resilience and interesting optical properties for the fabrication of stretchable and conformable reflective gratings;[20,21] this approach is called Supersonic Cluster Beam Implantation (SCBI).

Here, we report the fabrication by SCBI of stretchable Au-PDMS nanocomposites showing a stable plasmon peak shift up to 180 nm induced by mechanical deformation. We characterized the influence of cluster density on the plasmon frequency shift upon stretching, with particular attention to the evolution of the optical properties with increasing number of deformation cycles and on the conditions to obtain stable and reproducible performances upon a large number of stretching cycles.

We fabricated Au-PDMS nanocomposites by implanting different quantities of neutral Au clusters with a size distribution as reported in Figs. 1(a) and 1(b) in PDMS substrates.[22]

[a)]Author to whom correspondence should be addressed. Electronic mail: pmilani@mi.infn.it

Neutral gold clusters were produced by a Pulsed Microplasma Cluster Source (PMCS) and accelerated for implantation in a supersonic expansion, as described in detail in Ref. 23. A PMCS schematically consists of a ceramic body with a cavity where a target gold rod, acting as a cathode, is sputtered by a localized electrical discharge ignited during the pulsed injection of an inert carrier gas (He or Ar) at high pressure (40 bars). The sputtered metal atoms from the target thermalize with the carrier gas and aggregate in the cavity forming metal clusters; the carrier gas-cluster mixture expands out of the PMCS through a nozzle into a low-pressure (10^{-4} mbar) expansion chamber, thus producing a highly collimated supersonic beam with a divergence lower than 1°.[23] The central part of the beam enters a second vacuum chamber (deposition chamber, at a pressure of about 10^{-5} mbar) through a skimmer and it impinges on a PDMS substrate supported by a motorized substrate holder. PDMS films were produced with a Sylgard 184 Elastomer Kit by mixing the base and the curing agent in a 10:1 ratio for about 15 min and by subsequently spin-coating the mixture on a rigid substrate for 60 s at 800 rpm, polymerization is performed with a 60 min annealing at 100 °C. This procedure produces PDMS membranes with a thickness of about 60 μm.

During cluster implantation, the holder displaces the substrate in the two directions orthogonal to the cluster beam axis, allowing the parallel fabrication of multiple samples with an area of 2 cm^2.[24] Supersonic expansion accelerates the clusters to a mean velocity of approximately 1000 $m \cdot s^{-1}$, meaning that the metal clusters are accelerated towards the polymeric substrate with a kinetic energy E_k of roughly 0.5 $eV \cdot atom^{-1}$.

The implanted Au clusters volume fraction (VF) (Au volume concentration) is defined as the ratio between the total volume of the metal clusters (the filler) and the volume of polymer, in which the clusters are implanted. Considering a homogeneously filled nanocomposite, this corresponds to the ratio between the equivalent thickness of the implanted nanoparticles and the thickness of the nanocomposite layer. This latter (nanoparticle implantation depth) is obtained by transmission electron microscopy (TEM) characterization (Fig. 1(c)). The equivalent thickness T_{eq} of nanoparticles implanted into the PDMS is obtained as follows: a half-masked hard substrate (e.g., silicon or glass) is placed close to the polymeric substrate during implantation so that the same amounts of nanoparticles are intercepted both by the substrate and the polymer. Nanoparticles intercepted by the hard substrate result in a nanostructured layer whose thickness can be measured, once the mask is removed, by AFM.[24] Samples with a volume fraction in the range of 22%–48% were produced.

LSPRs evolution upon stretching has been characterized for each sample by recording the absorbance spectra in the visible range, with a spectrophotometer (Jasco 7850). The samples were mounted on a custom-built, computer controlled motorized uniaxial stretcher. Each sample was stretched up to 50% for 5000 cycles. Spectra were acquired at regular elongation state after 1, 500, 1500, and 5000 cycles.

The typical behavior of the plasmon peak upon stretching is reported in Fig. 2(a) where we show the optical absorption spectra at different elongations for a nanocomposite filled with a 31% volume fraction: the applied strain causes a broadening of the spectrum accompanied by an absorbance reduction and by a marked LSPR shift toward larger wavelength. These effects are quantitatively reported in detail in Fig. 2(b), where LSPR wavelength and absorbance are plotted versus stretching: the LSPR peak

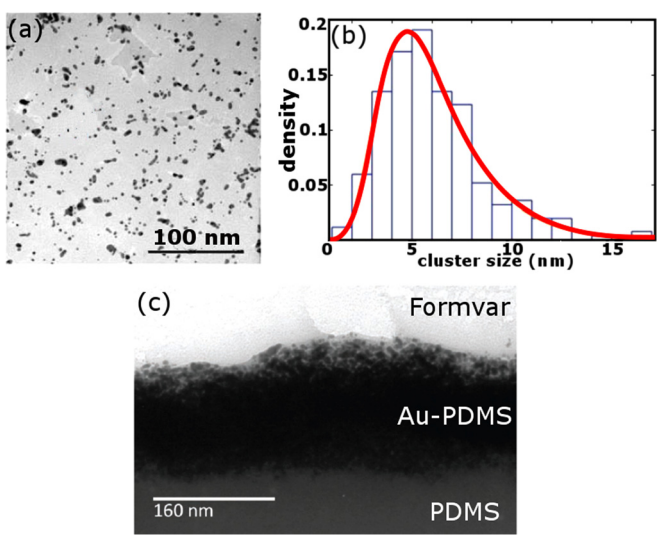

FIG. 1. (a) Transmission electron microscopy (TEM) micrograph of Au clusters deposited on a Formvar grid for the measurement of size distribution. (b) Au cluster size distribution obtained from TEM analysis and log-normal fit (red curve): the distribution is peaked at a value of 4.72 nm. (c) TEM image of a 300 nm-thick section of an Au-PDMS nanocomposite.

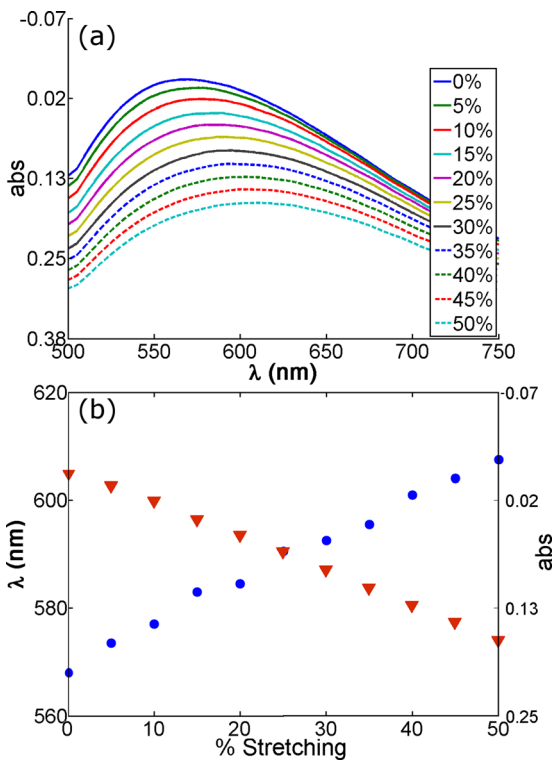

FIG. 2. (a) Absorbance spectra acquired at different applied strains. Absorbances have been normalized as $-\log(I/I_{0\%})$, where I is the measured absorbance and $I_{0\%}$ is the absorbance of the peak recorded in the non-stretched sample. (b) Plasmon peak wavelength (blue dots) and its corresponding absorbance (red triangles) versus strain. The nanocomposite VF is 31%.

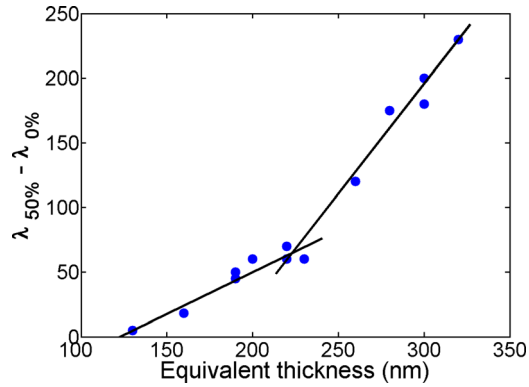

FIG. 3. Shifts of the surface plasmon resonance as a function of the nanocomposite volume fraction for a uniaxial deformation of 50% of the original dimension.

wavelength increases of about 40 nm, while its absorbance reduces of about 0.3 a.u. during a stretching cycle.

Most of the works reported in the literature analyze nanocomposites made from nanoparticle monolayer embedded in a polymeric substrate:[11–13] Cataldi *et al*. found that a stain of 20% causes a 70 nm absorbance peak redshift[11] and Zhu *et al*. found a redshift of 47 nm caused by 37% applied strain.[13]

According to the Maxwell-Garnett theory,[25] the LSPR redshift can be due to both an increase in cluster dimensions and an increase in nanocomposite filling factor.[4] When an elastomer is stretched in one direction, it is simultaneously compressed in the one perpendicular to that of the applied strain.[11,12] The compression degree depends on elastomer Poisson ratio: PDMS has a Poisson ratio of 0.5, so a 50% uniaxial stretching causes a 25% compression inducing a nanoparticle rearrangement and aggregation.[11]

The reduction of absorbance that we observe may be mainly due the reduction of the nanocomposite thickness upon stretching, while the nanoparticle volume fraction does not change. The quantification of the thickness change is difficult to obtain, since the nanocomposite Young's modulus is significantly different from that of the pristine elastomer, as discussed in detail in Ref. 26.

In our system, there is another aspect contributing to the redshift upon stretching: recently, it has been shown that SCBI produces a degradation to chains of low molar mass in the polymeric matrix and the formation of empty volumes.[27] Mechanical deformations can induce the reduction of the empty volumes and, as a consequence, the increase the nanocomposite filling factor.

SCBI has an interesting advantage compared to other nanocomposite production techniques: it allows the direct fabrication of systems with a well-controlled cluster VF over a wide range of values, reaching volume fractions that cannot be obtained with traditional approaches. This provides the possibility to study the influence of VF on the plasmonic behavior in regimes not yet explored. Figure 3 reports the peak wavelength shift for different samples with increasing volume fractions after a 50% stretching cycle.

The strain causes, for all the samples, an increase in peak redshift, as the VF increases, up to roughly 220 nm with a uniaxial deformation of 50%; these values are significantly larger than those reported in the literature for stretchable nanocomposites.[11–13] We observe two different linear trends, with the slope change occurring in correspondence of a volume fraction of about 33%. Several observations suggest that at this VF the cluster-assembled layer buried in the elastomer starts to emerge at the surface, causing a different packing of the nanoparticle upon further deposition.[22] This may reflect in a change of nanoparticle packing and rearrangement and hence optical response upon stretching.

The arrangement of nanoparticles embedded in an elastomeric matrix is affected by mechanical deformations: nanoparticles reorganize upon stretching thus influencing the electrical and optical properties of the nanocomposite.[20,28]

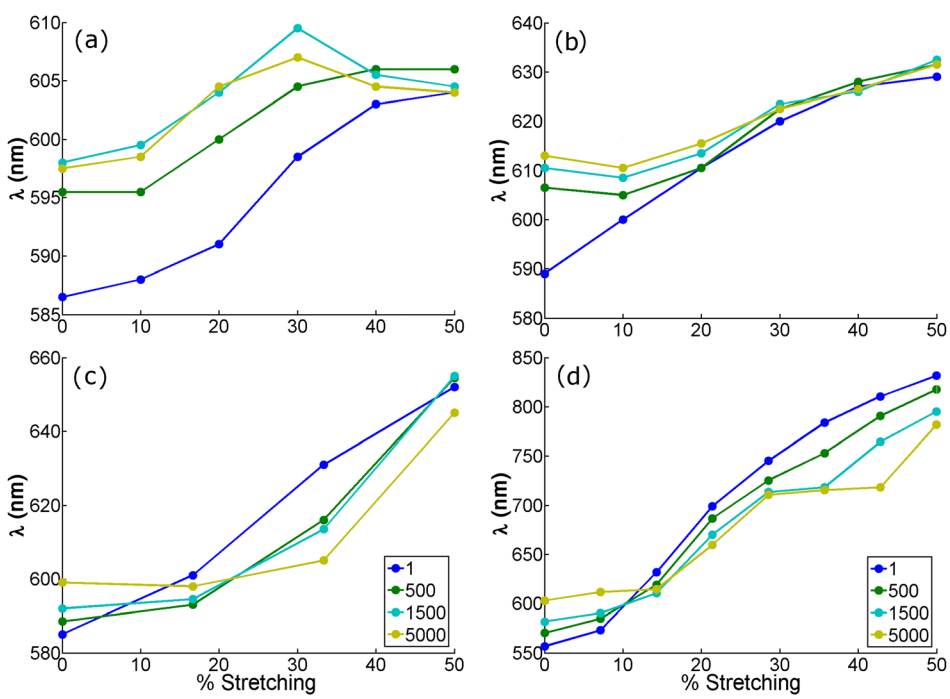

FIG. 4. Evolution of the wavelength of the plasmon peak for an increasing number of stretching cycles for samples with different cluster volume fractions: (a) 24%; (b) 28%; (c) 35%; (d) 45%.

For this reason, it is necessary to characterize the behavior of the plasmonic nanocomposite upon cyclical stretching to check for its stability. Figure 4 reports the optical response evolution at an increasing number of cycles up to 5000 for samples with different volume fractions.

In all the nanocomposites, the plasmonic shift behavior evolves with the number of stretching cycles: it is instable below 500 cycles, then the plasmon shift stabilizes and the curves acquired after 1500 and 5000 cycles tend to overlap within few nanometers. Again we observe a significant influence of the cluster volume fraction with two different regimes below and above a VF of roughly 30%.

More specifically, the 24% VF sample (Fig. 4(a)) shows an initial shift of about 17 nm upon 50% deformation decreasing substantially as the number of cycles increases: after 5000 cycles, it is reduced to about 6 nm. Moreover, the dependence of the plasmonic shift upon deformation is non-monotonic. A similar behavior, although less irregular, is observed for the 28% VF sample (Fig. 4(b)).

A significantly different trend is observed in nanocomposites with a volume fraction superior to 33%. In both the examples reported (Figs. 4(c) and 4(d)), even after 5000 cycles, a substantial plasmon peak position dependence on strain is preserved, the shift is stable, and it amounts at 46 and 179 nm for the 35% and 45% VF samples, respectively. These two shift values are about 32% lower than the ones acquired at the first cycle.

SPR peak shift induced by stretching can be explained by considering that clusters embedded in the matrix rearrange due to polymer deformation, causing their reciprocal distances to change. Aggregation and coagulation are favored if clusters have high mobility in the matrix.[19] For large VF, the mobility is reduced, especially for those nanoparticles above the matrix surface, thus increasing the nanocomposite behavior stability.

In summary, we demonstrated the fabrication of Au-PDMS plasmonic nanocomposites by implanting neutral gold clusters in a PDMS matrix by supersonic cluster beam implantation. The nanocomposites show a plasmon peak shift upon deformation depending on the implanted clusters volume fraction with a stable red shift up to 180 nm with a deformation of 50%. Cyclic stretching induces a rearrangement and reorganization of the embedded clusters affecting the plasmonic behavior. This results in an almost complete disappearance of the plasmon shift for samples with volume fractions below 30% after few hundreds of stretching cycles. For larger volume fractions, a substantial plasmon shift remains and stabilizes after a suitable mechanical post deposition treatment, providing the evidence that nanocomposites produced by SCBI can be used as mechanically tunable optical filters or as components for stretchable optical devices.

We acknowledge Cristian Ghisleri for insightful discussions.

[1]U. Kreibig and M. Vollmer, *Optical Properties of Metal Clusters* (Springer-Verlag, 1995).
[2]N. I. Grigorchuk, J. Phys. Chem. C **116**, 23704 (2012).
[3]M. K. Kinnan and G. Chumanov, J. Phys. Chem. C **114**, 7496 (2010).
[4]S. K. Ghosh and T. Pal, Chem. Rev. **107**, 4797 (2007).
[5]J. Homola, Anal. Bioanal. Chem. **377**, 528 (2003).
[6]T.-H. Meen, J. Tsai, S. Chao, Y. Lin, T. Wu, T. Chang, L. Ji, W. Water, W. Chen, I. Tang, and C. Huang, Nanoscale Res. Lett. **8**, 450 (2013).
[7]S. Pillai, K. R. Catchpole, T. Trupke, and M. A. Green, J. Appl. Phys. **101**, 093105 (2007).
[8]V. J. Sorger, R. F. Oulton, R. M. Ma, and X. Zhang, MRS Bull. **37**, 728 (2012).
[9]M. Millyard, F. M. Huang, R. White, E. Spigone, J. Kivioja, and J. J. Baumberg, Appl. Phys. Lett. **100**, 073101 (2012).
[10]M. K. Hedayati, A. U. Zillohu, T. Strunskus, F. Faupel, and M. Elbahri, Appl. Phys. Lett. **104**, 041103 (2014).
[11]U. Cataldi, R. Caputo, Y. Kurylyak, G. Klein, M. Chekini, C. Umeton, and T. Bürgi, J. Mater. Chem. C **2**, 7927 (2014).
[12]Y. F. Chiang, C. W. Chen, C. H. Wang, C. Y. Hsieh, Y. T. Chen, H. Y. Shih, and Y. F. Chen, Appl. Phys. Lett. **96**, 041904 (2010).
[13]X. Zhu, L. Shi, X. Liu, J. Zi, and Z. Wang, Nano Res. **3**, 807 (2010).
[14]W. Caseri, Macromol. Rapid Commun. **21**, 705 (2000).
[15]F. Faupel, V. Zaporojtchenko, H. Greve, U. Schurmann, V. S. K. Chakravadhanula, C. Hanisch, A. Kulkarni, A. Gerber, E. Quandt, and R. Podschun, Contrib. Plasma Phys. **47**, 537 (2007).
[16]H. Takele, A. Kulkarni, S. Jebril, V. S. K. Chakravadhanula, C. Hanisch, T. Strunskus, V. Zaporojtchenko, and F. Faupel, J. Phys. D: Appl. Phys. **41**, 125409 (2008).
[17]K. Vanherck, T. Verbiest, and I. Vankelecom, J. Phys. Chem. C **116**, 115 (2012).
[18]I. Pastoriza-Santos, J. Pérez-Juste, G. Kickelbick, and L. Liz-Marzán, J. Nanosci. Nanotechnol. **6**, 453 (2006).
[19]Y. Kim, J. Zhu, B. Yeom, M. Di Prima, X. Su, J. G. Kim, S. J. Yoo, C. Uher, and N. A. Kotov, Nature **500**, 59 (2013).
[20]C. Ghisleri, M. Siano, M. A. C. Potenza, L. Ravagnan, and P. Milani, Laser Photonics Rev. **7**, 1020 (2013).
[21]C. Ghisleri, M. A. C. Potenza, L. Ravagnan, A. Bellacicca, and P. Milani, Appl. Phys. Lett. **104**, 061910 (2014).
[22]G. Corbelli, Ph.D. thesis, Università degli Studi di Milano, 2011.
[23]P. Piseri, H. V. Tafreshi, and P. Milani, Curr. Opinion Solid State Mater. Sci. **8**, 195 (2004).
[24]C. Ghisleri, F. Borghi, L. Ravagnan, A. Podestà, C. Melis, L. Colombo, and P. Milani, J. Phys. D: Appl. Phys. **47**, 015301 (2014).
[25]J. C. Maxwell Garnett, Philos. Trans. R. Soc. London, Ser. A **205**, 237 (1904).
[26]F. Borghi, C. Melis, C. Ghisleri, A. Podestà, L. Ravagnan, L. Colombo, and P. Milani, Appl. Phys. Lett. **106**, 121902 (2015).
[27]R. Cardia, C. Melis, and L. Colombo, J. Appl. Phys. **113**, 224307 (2013).
[28]G. Corbelli, C. Ghisleri, M. Marelli, P. Milani, and L. Ravagnan, Adv. Mater. **23**, 4504 (2011).